ACS APPLIED MATERIALS & INTERFACES

Research Article

www.acsami.org

Patterned Fluoropolymer Barriers for Containment of Organic Solvents within Paper-Based Microfluidic Devices

Benny Chen, Philip Kwong, and Malancha Gupta*

Mork Family Department of Chemical Engineering and Materials Science, University of Southern California, Los Angeles, California 90089, United States

Supporting Information

ABSTRACT: In this study, we demonstrate for the first time the ability to pattern lipophobic fluoropolymer barriers for the incorporation of pure organic solvents as operating liquids within paper-based microfluidic devices. Our fabrication method involves replacing traditional wax barriers with fluoropolymer coatings by combining initiated chemical vapor deposition with inhibiting transition metal salt to pattern the polymer. Multiple techniques for patterning the transition metal salt are tested including painting, spray coating, and selective wetting through the use of a photoresist. The efficacy of the barrier coatings to contain organic solvents is found to be dependent on the conformality of the polymer deposited around the paper fibers. We demonstrate examples of the benefits provided by the containment of organic solvents in paper-based microfluidic applications including the ability to tune the separation of analytes by varying the operating solvent and by modifying the channel region of the devices with additional polymer coatings. The work exhibited in this paper has the potential to significantly expand the applications of paper-based microfluidics to include detection of water insoluble analytes. Additionally, the generality of the patterning process allows this technique to be extended to other applications that may require the use of patterned hydrophobic and lipophobic regions, such as biosensing, chemical detection, and optics.

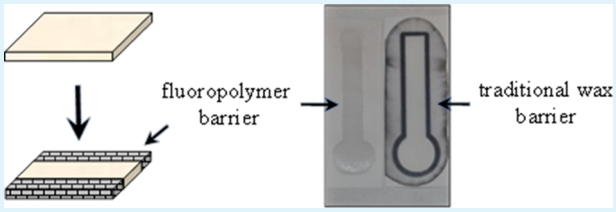

KEYWORDS: *microfluidics, polymers, coatings, patterning, separations, fluoropolymer*

INTRODUCTION

Paper-based microfluidic devices are an attractive option for rapid low-cost diagnostics because of numerous advantages including portability,[1] ease of use,[2] and limited requirements for operation.[3] Recent developments have expanded the available operations for paper-based microfluidic platforms to include mixing,[4] separation of analytes,[5,6] biosensing,[7] and fluid manipulation using integrated valves and fluidic diodes.[8] Paper-based microfluidic devices operate using capillary action to drive liquid flow, which is typically directed by wax barriers.[9,10] Attempts at using other media to direct the flow of liquids such as hydrophobic photoresists,[11] polymer yarns,[12] and silk[13] have also been explored. However, these methods use hydrophobic barriers that are vulnerable to effects such as dissolution, solvent diffusion, or swelling by organic solvents that ultimately restricts the possible operating liquids to aqueous solvents.

The use of organic solvents within paper-based assays has been challenging because of the difficulty of creating lipophobic barriers.[14] Expanding the operating liquids used in paper-based microfluidic devices to include organic solvents could unlock several advantages over traditional aqueous solvents. For example, utilizing organic solvents could expand the applications of these devices for the processing and analysis of water insoluble chemicals, including pharmaceutical drugs,[15] and chemical warfare agents and pesticides, such as organophosphates.[16−18] These assays may require sequential or timed multi-step reactions, interfacial reactions, or separation of other hydrophobic contaminants. By utilizing lipophobic barriers that are compatible with organic solvents, these assays could potentially be translated onto paper-based microfluidic devices by directing and manipulating liquid flow. The use of organic solvents would also allow for additional modification and tuning of both the mobile and stationary phases, yielding highly adaptable platforms.

Fluoropolymers have been known to exhibit desirable properties as a barrier material, including lipophobicity,[19,20] as well as excellent mechanical, thermal, and chemical stability.[21,22] For example, fluoropolymers have been used as the bulk material to replace poly(dimethylsiloxane) (PDMS) to fabricate chemically robust microfluidic devices.[23−25] Additionally, we have recently shown that initiated chemical vapor deposition (iCVD) can be used to deposit fluoropolymer coatings of poly(1*H*,1*H*,2*H*,2*H*-perfluorodecyl acrylate) (PPFDA) onto PDMS microfluidic devices to act as lipophobic barriers that prevent the diffusion of organic solvents.[26] The patterning of fluoropolymers has led to advancements in fields, such as biosensing,[22] pH-sensing,[27] and optical device fabrication.[28] However, the current techniques for patterning fluoropolymers, such as directed plasma exposure[29] or ion bombardament,[22]

Received: September 20, 2013
Accepted: November 22, 2013
Published: November 27, 2013

and microcontact printing,[27] are generally limited to planar substrates. In this paper, we demonstrate several methods for patterning thin conformal PPFDA coatings onto porous substrates to replace traditional wax barriers used in paper-based microfluidic devices, allowing for the containment of both aqueous and organic solvents without dissolution or swelling of the barrier. The fluoropolymer was patterned using iCVD in combination with transition metal salts, which are able to selectively inhibit the deposition of polymer.[30] The iCVD technique is a solvent-free coating process that uses a heated filament to decompose initiator molecules into radical species that react with monomer molecules to begin free radical polymerization. The solventless nature of the iCVD process alleviates common issues caused by solvents during polymer processing, such as dewetting and clogging, and has been previously used to conformally coat a variety of non-planar substrates, including electrospun fiber mats[31,32] and silicon nanotrenches.[33] In addition, the iCVD technique allows for sequential deposition of conformal, functional polymer coatings onto porous materials.[6] We evaluate the resolution of the following three patterning methods for the application of the transition metal salt inhibitor: painting, spray coating, and selective wetting through the use of a photoresist. Previous attempts at patterning polymers onto porous substrates via iCVD using physical masking have proven unsuccessful due to the large mean-free path of the reactant vapors.[30] While other patterning methods have been successfully combined with iCVD, such as electron-beam lithography[34,35] and capillary force lithography,[36] these methods are generally limited to planar substrates. In contrast, the use of transition metal salts allows us to pattern fluoropolymer barrier coatings through the depth of porous chromatography paper by selectively inhibiting the deposition of polymer.

We demonstrate that the fluoropolymer barrier coatings can be used to improve separation processes within paper-based microfluidic devices. The fluoropolymer barrier coatings enable the modification of the mobile phase using various organic solvents to tune the separation of water insoluble analytes. Additionally, the use of organic operating liquids allows for modification of the stationary phase with organic polymer coatings that are incompatible with aqueous systems due to their hydrophobicity. The use of polymer coatings to modify stationary phases in column chromatography has shown an abundance of utility, such as the ability to facilitate hydrophobic interaction chromatography[37,38] and size-based separation,[39,40] but has only recently been demonstrated for aqueous-based paper-based microfluidic applications using electrostatic interactions.[6] In this study, we use the iCVD process to modify the channels of our devices with polymer coatings to further tune the separation of analytes using interactions such as hydrogen bonding and π-stacking. The iCVD process is ideal for modifying paper-based microfluidic devices due to its ability to conformally coat porous substrates without compromising their morphology[6,30,41] as maintaining the porous nature of the paper is essential because of its critical role in facilitating capillary-force driven flow.

RESULTS AND DISCUSSION

Paper-based microfluidic channels were fabricated by patterning fluoropolymer PPFDA barrier coatings onto Grade 1 Whatman chromatography paper using the iCVD process in combination with copper(II) chloride ($CuCl_2$), as shown in Figure 1a. A solution of $CuCl_2$, which acted to inhibit polymer deposition,[30] was applied using three different techniques: painting, spray coating, and selective wetting through the use of a hydrophobic photoresist. After the transition metal salt was applied, the sample was coated using the iCVD process with 50 nm of PPFDA (as measured on a reference silicon wafer using in situ interferometry). After the deposition of the PPFDA barrier coating, the channels were washed with water and methanol to remove the $CuCl_2$ salt. The PPFDA coating was conformal around the paper fibers and did not occlude the pores of the paper, as shown in the scanning electron micrographs of the paper before and after deposition (Figure 1b). The resolution of each salt application technique was evaluated by comparing the dimensions of a resultant fluoropolymer pattern to an intended design. A tapered triangular channel was used as the intended design to evaluate the resolution as a function of channel width. For all three methods of salt application, the

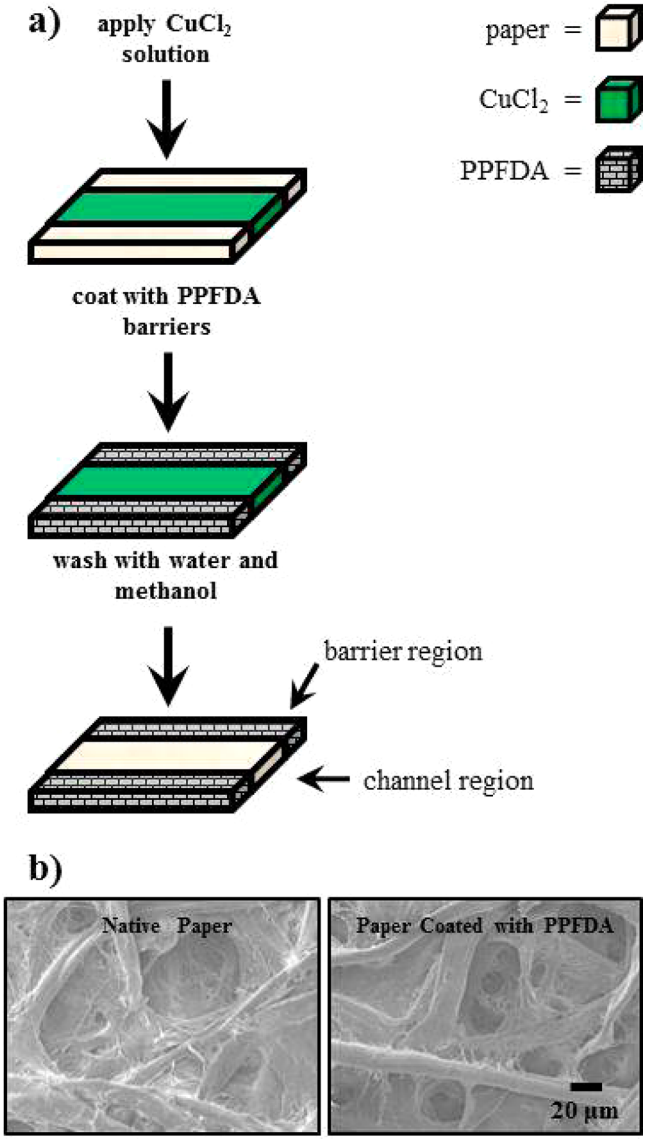

Figure 1. (a) Schematic representation of the device fabrication process. $CuCl_2$ is applied to the chromatography paper by painting, spray coating, or photolithography, yielding selective deposition of PPFDA by iCVD in the areas free of $CuCl_2$. The salt is then removed to yield the final device. (b) Scanning electron micrographs of chromatography paper before and after deposition of 440 nm of PPFDA.

resultant fluoropolymer pattern was larger than the intended design and the deviation was found to be independent of channel width over the range tested. Painting was performed by brushing a solution of $CuCl_2$ in methanol and diethyl ether onto the paper. Methanol was selected to ensure the dissolution of the $CuCl_2$ salt, while diethyl ether was selected to provide a fast evaporation rate for greater control over the application of the salt. Even while demonstrating extreme care when painting, this technique was the least consistent, yielding an average deviation of 0.80 ± 0.26 mm (Supporting Information Table S1) between the intended channel width and the actual channel width. When attempting to pattern large areas or multiple devices simultaneously, a technique such as spray coating is preferable since it is capable of rapidly applying salt solution over large areas. We tested the resolution of this technique by spraying a solution of $CuCl_2$ in methanol and diethyl ether onto the paper through a physical mask. The resultant deviation between the intended channel width and the actual channel width was found to be 0.46 ± 0.10 mm (Supporting Information Table S2), which is a significant improvement when compared to painting. Although the spray coating technique was able to produce samples quickly and with improved resolution, it should be noted that this technique required significantly more $CuCl_2$ because of the loss of the solution onto the mask and to the surrounding area. For applications that require higher resolution, a photolithographic approach can be used. In this method, patterns were produced by first conformally coating the paper fibers with the hydrophobic photoresist poly(*ortho*-nitrobenzyl methacrylate) (P*o*NBMA) using the iCVD process.[41] The photoresist was then selectively exposed to UV light to generate patterned hydrophilic areas, which were then wet with an aqueous solution of $CuCl_2$. The conformal nature of the iCVD process ensured that the patterned photoresist did not occlude the pores of the paper, allowing for the subsequent fluoropolymer deposition to infiltrate the entire thickness of the paper. Using this photolithographic process, we were able to produce patterns that deviated from the intended channel width by 0.33 ± 0.10 mm (Supporting Information Table S3). While the deviations in the painting and spray coating methods are likely the result of the $CuCl_2$ solution bleeding outside the intended area, the use of a hydrophobic photoresist prevents bleeding. The deviation associated with the use of a photoresist is instead attributed to undercutting of the photoresist during exposure. It is important to note that other patterning techniques for applying the salt solutions may yield better resolution or scalability, such as inkjet printing;[42] however, this method requires surfactants and optimization to prevent clogging of printer heads. Since the painting technique required less $CuCl_2$ than spray coating and was less cumbersome than photolithography, we used the painting method for the remainder of our studies.

For the deposition of the PPFDA barrier coatings, two criteria must be met to effectively fabricate the devices: (1) the PPFDA coating in the barrier region must be conformal around the paper fibers, otherwise the uncoated areas may cause solvent to bleed through the barrier, and (2) the deposition of PPFDA in the channel region must be inhibited to prevent unpredictable wetting and decreased device performance. While the first criterion is more easily satisfied at higher coating thicknesses, the second criterion is more easily satisfied at lower coating thicknesses since the ability of transition metal salts to inhibit the deposition of iCVD coatings has been shown to decrease as greater amounts of polymer are deposited. This decrease in inhibition was hypothesized to be caused by the formation of a layer of deactivated precursor molecules that shields the transition metal salt from deactivating additional precursor molecules.[30] To systematically determine the PPFDA coating thicknesses that fulfilled both criteria, X-ray photoelectron spectroscopy (XPS) was used to analyze the amount of PPFDA in both the barrier region (Figure 2a) and in the channel region (Figure 2b) as a function of the coating thickness as measured on a reference silicon wafer. The XPS spectra of the paper surface showed an increasing fluorine intensity at 686 eV with increasing coating thickness in both the barrier and channel regions which is indicative of an increasing amount of PPFDA on the surface. XPS probes approximately the top 5 nm of the surface and therefore the weight fraction of the PPFDA on the surface relative to cellulose can be estimated by comparing the fluorine to carbon ratio on the surface of the devices to a surface of homopolymer PPFDA (Table 1). If the

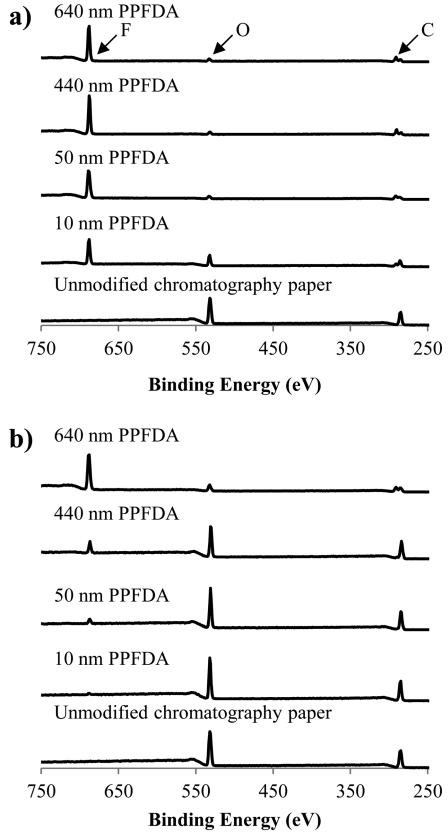

Figure 2. XPS spectra showing the chemical composition of (a) the barrier regions and (b) the channel regions of devices with different thicknesses of deposited PPFDA.

Table 1. Weight Fraction of PPFDA in the Barrier and Channel Regions of the Paper Devices

polymer thickness on reference silicon wafer (nm)	weight fraction of PPFDA in barrier regions	weight fraction of PPFDA in channel regions
10	0.68	0.03
50	0.99	0.08
440	0.98	0.17
640	0.99	0.85

coating was too thin, areas of cellulose remained exposed as indicated by a low PPFDA weight fraction. For example, when 10 nm of coating was deposited, the PPFDA weight fraction within the barriers was only 0.68, resulting in barriers that were unable to contain hexane within the channel (Figure 3a). This

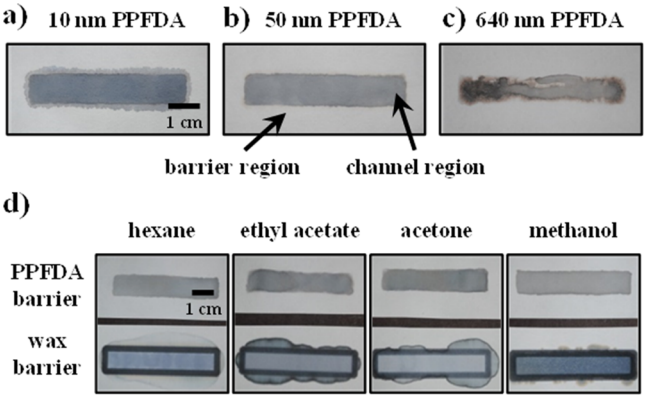

Figure 3. Images of paper-based microfluidic devices after applying organic solvents containing dye for visualization. Fluoropolymer barriers (a) are unable to contain hexane with a 10 nm thick PPFDA coating, (b) are able to successfully contain hexane with a 50 nm thick PPFDA coating, and (c) have non-uniform wetting with a 640 nm thick PPFDA coating. (d) Fluoropolymer barriers made with a 50 nm thick PPFDA coating succeed at containing a wide variety of organic solvents whereas traditional wax barriers fail.

XPS data also indicates that the thickness of PPFDA on the paper was lower than that measured on the reference silicon wafer, which is likely due to the fibrous nature of the paper. When the coating thickness was increased to 50 nm or more, the PPFDA weight fraction within the barriers remained steady at approximately 0.98–0.99 indicating at least 5 nm of conformal coating, and yielded barriers that could contain hexane (Figure 3b). However, as we deposited thicker coatings, the transition metal salt was unable to conformally inhibit the deposition of polymer, which resulted in a significant increase in the PPFDA weight fraction within the channel. As a result, 640 nm thick coatings showed non-uniform wetting of hexane within the channel region (Figure 3c). To further evaluate the amount of PPFDA in the barrier and channel regions and the corresponding wetting properties, we used contact angle goniometry to measure the static contact angles of water on the top and bottom sides of our samples (Table 2). The contact angles on both regions approached the contact angle on a control sample of PPFDA (1 μm thick) deposited on

Table 2. Water Contact Angles on Both the Top and Bottom of the Barrier and Channel Regions of the Paper Devices

polymer thickness on reference silicon wafer (nm)		contact angle in barrier regions (deg)	contact angle in channel regions (deg)
10	top	124.5 ± 0.9	0.0 ± 0.0
	bottom	125.9 ± 4.0	0.0 ± 0.0
50	top	148.1 ± 1.2	0.0 ± 0.0
	bottom	145.4 ± 3.0	0.0 ± 0.0
440	top	147.3 ± 1.0	106.0 ± 7.4
	bottom	149.9 ± 4.9	110.9 ± 4.1
640	top	154.0 ± 1.2	154.2 ± 0.6
	bottom	155.6 ± 2.6	154.9 ± 2.9

unpatterned paper (154.1° ± 2.7°), which was consistent with the XPS data. The top and bottom sides of the paper exhibited similar contact angles even at low deposition thicknesses, confirming that the PPFDA coating was conformal through the depth of the Grade 1 Whatman chromatography paper (180 μm thick). We also measured the water contact angle after deposition of PPFDA onto Grade 3 Whatman chromatography paper (360 μm thick), and found that the contact angles on the top and bottom sides of the paper were identical within error. These results demonstrated that the deposition of PPFDA was highly conformal despite the tortuous nature of the paper and generated uniform wetting properties.

On the basis of our observations above, we deposited approximately 50 nm of PPFDA on all further paper-based microfluidic devices to effectively contain organic solvents. Although the channel regions contained a small amount of PPFDA, the resultant devices exhibited the same solvent wicking behavior as uncoated paper, indicating that this low amount of PPFDA did not significantly affect device performance. A comparison between the ability of the PPFDA barriers and traditional wax barriers to contain organic solvents with contrasting polarities (hexane, ethyl acetate, acetone, and methanol) is shown in Figure 3d. In all cases, the tested solvents were able to penetrate the traditional wax barriers, leading to undesirable flows. Conversely, the PPFDA barriers were able to successfully contain this wide variety of solvents. A full list of tested solvents can be found in Supporting Information Table S4.

The ability to use organic solvents in paper-based microfluidic devices allows for a variety of operations that are difficult or impossible with aqueous solvents, such as the chromatographic separation of lipophilic analytes. A common metric used to describe chromatographic separation is the retardation factor (R_f), which is defined as the distance travelled by the analyte relative to the distance travelled by the mobile phase. Higher R_f values exist when there is greater affinity between the analyte and the mobile phase, while lower R_f values exist when there is greater affinity between the analyte and the stationary phase. Thus, we can tune the R_f value of analytes by modifying either the mobile or stationary phase of the system, allowing for separation of a multi-component system. A simple demonstration of how the mobile phase can be tailored to yield specific degrees of separation is shown in Figure 4a where various compositions of methanol and water were used to control the R_f values of the lipophilic dyes Sudan Black B and Nile Red. An inset schematic in Figure 4a depicts the relative R_f values of Sudan Black B and Nile Red as the mobile phase is varied. As the relative amount of methanol decreased, the R_f value of Nile Red decreased more rapidly than Sudan Black B, resulting in a larger separation between the analytes. This observation can be explained by the greater affinity between Sudan Black B and methanol compared to the affinity between Nile Red and methanol. Although two lipophilic dyes were examined as model analytes, the ability to use organic solvents to affect the separation of a mixture of analytes is applicable to a wide variety of systems. Additionally, channels can be modified with functional polymer coatings that may be incompatible with aqueous systems due to their hydrophobicity in order to further tune the R_f value of analytes. For example, we modified our channels using iCVD by conformally pre-coating chromatography paper with copolymers composed of 4-vinyl pyridine (4VP) and ethylene glycol dimethacrylate (EGDMA) prior to

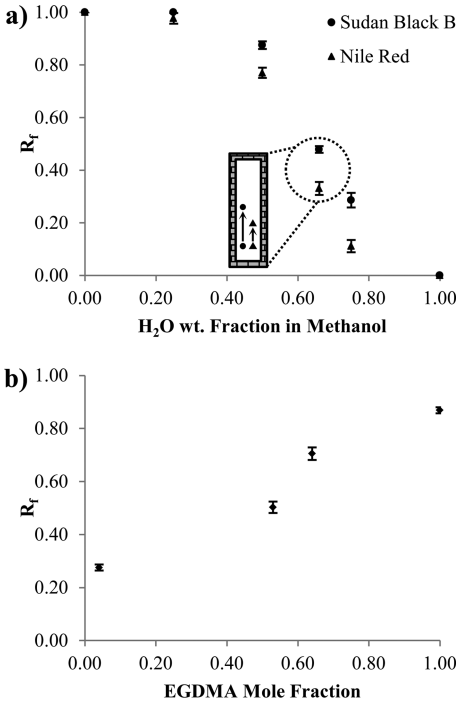

Figure 4. Graphs plotting retardation factors of (a) Sudan Black B and Nile Red in solvent blends of water and methanol on cellulose patterned with fluoropolymer barrier coatings (inset schematic represents R_f values of Sudan Black B and Nile Red) and (b) Sudan Black B in hexane on channels coated with copolymers composed of 4VP and EGDMA on devices patterned with fluoropolymer barrier coatings.

depositing the fluoropolymer barriers in order to tune the R_f value of Sudan Black B in hexane. The mole fraction of EGDMA in the copolymer coating was systematically varied between 0.04 and 1.00, as determined by XPS (Table 3). In addition to providing functionality, the EGDMA cross-linker also prevented dissolution of the copolymer coatings. The lowest R_f value of Sudan Black B was measured on an unmodified cellulose channel (0.22 ± 0.02), which we hypothesize to be due to the ability of cellulose to act as both a proton donor (OH···N) and acceptor (O···HN), resulting in greater affinity to the analyte Sudan Black B. The effect of the EGDMA mole fraction in the copolymer coating on the R_f values of Sudan Black B is shown in Figure 4b. When the stationary phase was modified with copolymer coatings composed mostly of 4VP (EGDMA mole fraction of 0.04), the R_f value increased slightly, which is likely due to weaker hydrogen bonding interactions between the 4VP moieties and Sudan Black B (N···HN) compared to cellulose and Sudan Black B, as well the inability of 4VP moieties to act as a proton donor. However, the weaker interactions may be offset by the presence of π-stacking interactions, leading to only a small net change in the R_f value. As the mole fraction of EGDMA increased, the R_f value monotonically increased, which we attribute to decreased attraction between Sudan Black B and the copolymer coating due to a reduction of π-stacking interactions. The effect of the copolymer on the R_f value of Nile Red showed a similar trend and thus resulted in minimal separation of the two dyes. Nevertheless, these results show that modifying the stationary phase with polymer coatings allows the R_f value of analytes to be tuned over a wide range, which can potentially improve the separation of multi-component systems.

Table 3. Mole Fraction of EGDMA in Copolymer Coating and Corresponding R_f Value of Sudan Black B with Hexane as the Mobile Phase

mole fraction of EGDMA	R_f
0.04	0.28 ± 0.01
0.53	0.50 ± 0.02
0.64	0.71 ± 0.02
1.00	0.87 ± 0.01

CONCLUSION

We have demonstrated the ability to use organic solvents within paper-based microfluidic devices by patterning fluoropolymer barriers using iCVD in conjunction with transition metal salts that inhibit polymer deposition. The patterning resolution of three different methods of applying the salt were compared, and it was revealed that selective wetting through use of a hydrophobic photoresist yielded the highest resolution. XPS was used to determine the amount of fluoropolymer coating necessary for optimal performance of the device. The efficacy of the fluoropolymer barrier coatings relied on the conformality of the coating around the paper fibers. However, depositing excess polymer jeopardized the ability of the transition metal salt to inhibit polymer deposition within the intended channel regions. We demonstrated the utility of using organic solvents in paper-based microfluidic applications by separating lipophilic dyes by controlling the composition of the operating solvent and by application of organic polymer coatings within the channels. Although we provided examples of applications using simple straight channels, the generality of our technique can be applied to more complex devices and can broaden the range of available applications for paper-based microfluidic devices by expanding the possible operating liquids. Additionally, our technique has the potential to advance current fields that employ the use of hydrophobic or lipophobic regions such as biosensing, chemical detection, and optics.

EXPERIMENTAL SECTION

1*H*,1*H*,2*H*,2*H*-Perfluorodecyl acrylate (PFDA) (SynQuest, 97 %), di-*tert*-butyl peroxide (Sigma Aldrich, 98 %), 4-vinyl pyridine (Sigma Aldrich, 95 %), ethylene glycol dimethacrylate (Sigma Aldrich, 98 %), *ortho*-nitrobenzyl methacrylate (*o*NBMA) (Polysciences, 95 %), copper(II) chloride (Sigma Aldrich, reagent Grade), Grade 1 chromatography paper (Whatman), Grade 3 chromatography paper (Whatman), pH 8 buffer (BDH, pH 8 ± 0.02), acetone (Macron, 99.5 %), acetonitrile (Mallinckrodt, 99.5 %), butanol (Mallinckrodt, 99.4 %), chloroform (Mallinckrodt, 99.9 %), cyclohexane (EMD, 99.99 %) diethyl ether (BDH, 99 %), dimethyl formamide (EMD, 99.8 %), dimethyl sulfoxide (Mallinckrodt, 99.8 %), ethanol (Koptec, 200 proof), ethyl acetate (Mallinckrodt, 99.5 %), hexane (EMD, 98.5 %), isopropanol (Macron, ACS Grade), methanol (Macron, absolute), tetrahydrofuran (Mallinckrodt, 99.0 %), toluene (J. T. Baker, 99.7 %), blue food coloring (McCormick), Sudan Black B (Sigma Aldrich, Biological Stain Commission certified), Nile Red (Sigma Aldrich, microscopy Grade), sulfuric acid (EMD, ACS Grade), and sodium hydroxide (Mallinckrodt, 98.8 %) were used as received without further purification.

To fabricate PPFDA barrier coatings, $CuCl_2$ was applied to chromatography paper and subsequently coated in a custom designed iCVD reactor chamber (GVD Corp, 250 mm diameter, 48 mm height). The deposition of PPFDA was performed at a constant pressure of 40 mTorr while the samples were maintained at 30 °C

using a backside recirculating chiller. The flow rates of the monomer, PFDA, and initiator, di-*tert*-butyl peroxide, were 0.4 and 3.9 sccm, respectively. During the deposition, a nichrome filament array (80 % Ni, 20 % Cr, Omega Engineering) inside the reactor was resistively heated to 250 °C to decompose the initiator molecules into free radicals. Polymerization occurred on the surface of the substrate via free radical polymerization. Polymer film thickness measurements on silicon wafers were obtained using a 633 nm helium−neon laser interferometer (Industrial Fiber Optics). Scanning electron microscopy (JEOL-7001) was used to confirm the conformal nature of the polymer coatings after deposition of 440 nm of PPFDA. Gold was sputtered onto the samples prior to imaging to prevent charging.

The $CuCl_2$ was applied prior to deposition of PPFDA using painting, spray coating, or selective wetting through use of a hydrophobic photoresist. Following the deposition of PPFDA, the $CuCl_2$ salt was removed by washing the samples with water, followed by methanol while the samples were still wet. The subsequent methanol wash was used to aid in removing the $CuCl_2$ salt, and also served to alleviate wrinkling effects that occurred during the evaporation of water. The samples were then allowed to dry in ambient conditions prior to analysis. The resolution of the patterning technique for each method of salt application was determined by comparing the width of an isosceles triangular mask with a base of 5 mm and a height of 50 mm to that of a final device dyed with a 50:1 by volume mixture of methanol and blue food coloring for visualization at nine equally distributed intervals from 1 mm to 5 mm from the apex along a line perpendicular to the base (Supporting Information Figure S1). The reported deviation is an average of these nine measurements across three samples per method with ± values representing one standard deviation.

Painted samples were patterned by applying approximately 80 μL/cm^2 of a 1:1 by volume mixture composed of diethyl ether and 4 M $CuCl_2$ in methanol onto chromatography paper using a standard 3/0 round paintbrush (Princeton Art & Brush Co.). A dark outline of the intended channel area was situated below the paper to act as a guide to be traced. Spray-coated samples were patterned by spraying a 4:1 by volume mixture composed of diethyl ether and 2 M $CuCl_2$ in methanol 50 times over physically masked chromatography paper using a household hand-operated spray bottle (FamilyMaid). After every 10 sprays, the samples were dried with a heat gun to evaporate excess methanol and diethyl ether. The selective wetting through the use of a hydrophobic photoresist was performed by first coating chromatography paper with approximately 25 nm of the photoresist P*o*NBMA using the iCVD process with a constant pressure of 50 mTorr, while the samples were maintained at 20 °C. The flow rates of the monomer, *o*NBMA, and initiator, di-*tert*-butyl peroxide, were 0.05 sccm and 0.7 sccm, respectively. After the photoresist was deposited, the paper was selectively exposed to 365 nm UV light (UVP, UVL-21) through a mask for 90 minutes. Afterwards, the sample was submerged in pH 8 buffer for 60 min, followed by a water rinse to remove the buffer and photoresist from the exposed areas. The paper was allowed to dry under ambient conditions, after which 40 μL/cm^2 of a 4 M aqueous solution of $CuCl_2$ was pipetted onto the exposed area.

Contact angle values for the unpatterned paper and the barrier and channel regions were measured with a goniometer (Ramé−Hart Model 290-F1) using 5 μL water droplets. Triplicate measurements were taken for each contact angle value. All unpatterned PPFDA paper samples were coated with 1 μm of polymer using the same reaction conditions as used for the barrier coatings.

To compare the fluoropolymer barriers to traditional wax barriers, wax toner was printed onto chromatography paper using a Xerox Phaser 8560N printer and subsequently melted through the depth of the paper using an oven set at approximately 180 °C for 3 minutes as described in previous studies.[9,10] Channels measuring 1 cm by 5 cm with PPFDA barriers were made by applying the $CuCl_2$ using the painting method. The evaluation of the ability of PPFDA barriers and traditional wax barriers to contain various solvents was performed by pipetting approximately 150 μL of a 0.2 mg/mL solution of Sudan Black B in each solvent into the channels followed by visual detection of whether the solvent bled through the barrier or exhibited irregular wetting behavior within the channel. Sudan Black B was dissolved in the solvents to provide greater contrast between the wetted and non-wetted areas.

The channel regions of devices measuring 1 cm by 5 cm were modified with polymer coatings by pre-coating chromatography paper with copolymers composed of 4-vinyl pyridine and ethylene glycol dimethacrylate using the iCVD process. For all depositions, the di-*tert*-butyl peroxide flow rate was 0.7 sccm, the filament temperature was 250 °C, and the samples were kept at 20 °C. The reaction conditions for each polymer coating are summarized in Table 4. PPFDA barriers were then subsequently patterned onto the coated paper as described above by applying $CuCl_2$ using the painting method.

Table 4. iCVD Experimental Conditions

flow rate of EGDMA (sccm)	flow rate of 4VP (sccm)	pressure (mTorr)	mole fraction of EGDMA in coating
0.2	7.8	500	0.04
0.2	5.8	325	0.53
0.2	3.5	200	0.64
0.2	0.0	50	1.00

The R_f values were determined by spotting a 0.4 % by weight methanolic solution of either Sudan Black B or Nile Red 1 cm from the bottom edge of the device. After the analyte dried, the device was inserted vertically into a glass chamber filled with solvent to a height of approximately 0.5 cm. The chamber was then immediately covered to reduce evaporation. When the mobile phase travelled at least 2 cm, the sample was removed from the chamber and the distances travelled by both the mobile phase and the analyte were measured to calculate the R_f value. The reported R_f values were an average of triplicate measurements using a new device for each measurement.

X-ray photoelectron spectroscopy (XPS) was performed using a Surface Science Instruments M-Probe spectrometer with a monochromatic Al Kα X-ray source. Survey spectra were averaged over 5 scans and were acquired at binding energies between 1 and 1000 eV with a resolution of 1 eV. Data analysis was performed using the ESCA25 Analysis Application software (V5.01.04). The relative amount of PPFDA on the surface of the paper devices was determined by comparing the relative carbon to fluorine atomic ratios, according to Supporting Information eq S1. The mole fraction of EGDMA in the copolymer coating was determined by comparing the relative carbon to nitrogen atomic ratios, according to Supporting Information eq S2, as measured on a reference silicon wafer.

■ ASSOCIATED CONTENT

Ⓢ Supporting Information

Figure defining the variables used to perform resolution analysis, tables showing the dimensions of the intended and patterned regions and the deviations for painting, spray coating, and photolithography, ability of wax barries and fluoropolymer barriers to contain solvents, determination of relative amount of PPFDA, and determination of copolymer composition. This material is available free of charge via the Internet at http://pubs.acs.org.

■ AUTHOR INFORMATION

Corresponding Author

*E-mail: malanchg@usc.edu.

Notes

The authors declare no competing financial interest.

■ ACKNOWLEDGMENTS

This work was supported by the National Science Foundation Division of Civil, Mechanical, and Manufacturing Innovation Award Number 1069328, the Natural Sciences and Engineering

Research Council of Canada Scholarship (P.K.), and the Alfred Mann Institute at the University of Southern California (P.K.). We thank the Molecular Materials Research Center of the Beckman Institute of the California Institute of Technology for use of their XPS. Grade 3 Whatman chromatography paper was kindly provided by GE Healthcare.

REFERENCES

(1) Nie, Z.; Nijhuis, C. A.; Gong, J.; Chen, X.; Kumachev, A.; Martinez, A. W.; Narovlyansky, M.; Whitesides, G. M. *Lab Chip* **2010**, *10*, 477−483.
(2) Martinez, A. W.; Phillips, S. T.; Whitesides, G. M. *Proc. Natl. Acad. Sci. U. S. A.* **2008**, *105*, 19606−19611.
(3) Martinez, A. W.; Phillips, S. T.; Whitesides, G. M.; Carrilho, E. *Anal. Chem.* **2010**, *82*, 3−10.
(4) Osborn, J. L.; Lutz, B.; Fu, E.; Kauffman, P.; Stevens, D. Y.; Yager, P. *Lab Chip* **2010**, *10*, 2659−2665.
(5) Yang, X.; Forouzan, O.; Brown, T. P.; Shevkoplyas, S. S. *Lab Chip* **2012**, *12*, 274−280.
(6) Kwong, P.; Gupta, M. *Anal. Chem.* **2012**, *84*, 10129−10135.
(7) Su, S.; Ali, M. M.; Filipe, C. D. M.; Li, Y.; Pelton, R. *Biomacromolecules* **2008**, *9*, 935−941.
(8) Chen, H.; Cogswell, J.; Anagnostopoulos, C.; Faghri, M. *Lab Chip* **2012**, *12*, 2909−2913.
(9) Lu, Y.; Shi, W.; Jiang, L.; Qin, J.; Lin, B. *Electrophoresis* **2009**, *30*, 1497−1500.
(10) Carrilho, E.; Martinez, A. W.; Whitesides, G. M. *Anal. Chem.* **2009**, *81*, 7091−7095.
(11) Martinez, A. W.; Phillips, S. T.; Carrilho, E.; Thomas, S. W.; Sindi, H.; Whitesides, G. M. *Anal. Chem.* **2008**, *80*, 3699−3707.
(12) Owens, T. L.; Leisen, J.; Beckham, H. W.; Breedveld, V. *ACS Appl. Mater. Interfaces* **2011**, *3*, 3796−3803.
(13) Bhandari, P.; Narahari, T.; Dendukuri, D. *Lab Chip* **2011**, *11*, 2493−2499.
(14) You, I.; Yun, N.; Lee, H. *ChemPhysChem* **2013**, *14*, 471−481.
(15) World Health Organization *Basic Tests for Pharmaceutical Dosage Forms*; World Health Organization: Geneva, Switzerland, 1991.
(16) Han, S.; Xue, Z.; Wang, Z.; Wen, T. B. *Chem. Commun.* **2010**, *46*, 8413−8415.
(17) O'Brien, R. D. *J. Biol. Chem.* **1956**, *219*, 927−931.
(18) Kim, J.-W.; Rainina, E. I.; Mulbry, W. W.; Engler, C. R.; Wild, J. R. *Biotechnol. Prog.* **2002**, *18*, 429−436.
(19) Yabu, H.; Takebayashi, M.; Tanaka, M.; Shimomura, M. *Langmuir* **2005**, *21*, 3235−3237.
(20) Mao, J.; Ni, P.; Mai, Y.; Yan, D. *Langmuir* **2007**, *23*, 5127−5134.
(21) Patri, M.; Hande, V. R.; Phadnis, S.; Deb, P. C. *Polym. Adv. Technol.* **2004**, *15*, 622−627.
(22) Jung, C.-H.; Hwang, I.-T.; Kuk, I.-S.; Choi, J.-H.; Oh, B.-K.; Lee, Y.-M. *ACS Appl. Mater. Interfaces* **2013**, *5*, 2155−2160.
(23) Rolland, J. P.; Van Dam, R. M.; Schorzman, D. A.; Quake, S. R.; DeSimone, J. M. *J. Am. Chem. Soc.* **2004**, *126*, 2322−2323.
(24) Taberham, A.; Kraft, M.; Mowlem, M.; Morgan, H. *J. Micromech. Microeng* **2008**, *18*, 064011.
(25) Begolo, S.; Colas, G.; Viovy, J.-L.; Malaquin, L. *Lab Chip* **2011**, *11*, 508−512.
(26) Riche, C. T.; Marin, B. C.; Malmstadt, N.; Gupta, M. *Lab Chip* **2011**, *11*, 3049−3052.
(27) Prissanaroon, W.; Brack, N.; Pigram, P. J.; Hale, P.; Kappen, P.; Liesegang, J. *Synth. Met.* **2005**, *154*, 105−108.
(28) Tamura, H.; Kojima, R.; Usui, H. *Appl. Opt.* **2003**, *42*, 4008−4015.
(29) Vargo, T. G.; Calvert, J. M.; Wynne, K. J.; Avlyanov, J. K.; MacDiarmid, A. G.; Rubner, M. F. *Supramol. Sci.* **1995**, *2*, 169−174.
(30) Kwong, P.; Flowers, C. A.; Gupta, M. *Langmuir* **2011**, *27*, 10634−10641.
(31) Ma, M.; Mao, Y.; Gupta, M.; Gleason, K. K.; Rutledge, G. C. *Macromolecules* **2005**, *38*, 9742−9748.
(32) Ma, M.; Gupta, M.; Li, Z.; Zhai, L.; Gleason, K. K.; Cohen, R. E.; Rubner, M. F.; Rutledge, G. C. *Adv. Mater.* **2007**, *19*, 255−259.
(33) Tenhaeff, W. E.; McIntosh, L. D.; Gleason, K. K. *Adv. Funct. Mater.* **2010**, *20*, 1144−1151.
(34) Im, S. G.; Kim, B.-S.; Lee, L. H.; Tenhaeff, W. E.; Hammond, P. T.; Gleason, K. K. *Macromol. Rapid Commun.* **2008**, *29*, 1648−1654.
(35) Mao, Y.; Felix, N. M.; Nguyen, P. T.; Ober, C. K.; Gleason, K. K. *J. Vac. Sci. Technol. B* **2004**, *22*, 2473−2478.
(36) Im, S. G.; Bong, K. W.; Kim, B.-S.; Baxamusa, S. H.; Hammond, P. T.; Doyle, P. S.; Gleason, K. K. *J. Am. Chem. Soc.* **2008**, *130*, 14424−14425.
(37) Chang, J.-P.; El Rassi, Z.; Horváth, C. *J. Chromatogr.* **1985**, *319*, 396−399.
(38) Hjertén, S.; Mohammad, J.; Eriksson, K.-O.; Liao, J.-L. *Chromatographia* **1991**, *31*, 85−94.
(39) Desilets, C. P.; Rounds, M. A.; Regnier, F. E. *J. Chromatogr.* **1991**, *544*, 25−39.
(40) Sing, Y. L. K.; Kroviarski, Y.; Cochet, S.; Dhermy, D.; Bertrand, O. *J. Chromatogr.* **1992**, *598*, 181−187.
(41) Haller, P. D.; Flowers, C. A.; Gupta, M. *Soft Matter* **2011**, *7*, 2428−2432.
(42) Thomas, S. W.; Chiechi, R. C.; LaFratta, C. N.; Webb, M. R.; Lee, A.; Wiley, B. J.; Zakin, M. R.; Walt, D. R.; Whitesides, G. M. *Proc. Natl. Acad. Sci. U. S. A.* **2009**, *106*, 9147−9150.